Exothermic Isomerization Reaction in a Reactive Flash: Steady-State Behavior

ARTICLE *in* INDUSTRIAL & ENGINEERING CHEMISTRY RESEARCH · MAY 2005

Impact Factor: 2.59 · DOI: 10.1021/ie0488748

3 AUTHORS:

Richard Lakerveld
The Hong Kong University of Science and Tec…
27 PUBLICATIONS **203** CITATIONS
SEE PROFILE

Costin Sorin Bildea
University Politehnica of Bucharest, Buchare…
145 PUBLICATIONS **851** CITATIONS
SEE PROFILE

Cristhian Almeida-Rivera
Organisation For The Prohibition Of Chemica…
34 PUBLICATIONS **196** CITATIONS
SEE PROFILE

Exothermic Isomerization Reaction in a Reactive Flash: Steady-State Behavior

Richard Lakerveld, Costin Sorin Bildea,* and Cristhian P. Almeida-Rivera

Delft University of Technology, Julianalaan 136, 2628 BL Delft, The Netherlands

The paper addresses the steady-state behavior of a reactive flash, characterized by an exothermic isomerization reaction with first-order kinetics and a light-boiling reactant. The dimensionless model distinguishes between the state variables, control parameters, and system properties. The combination of state multiplicity and feasibility boundaries corresponding to no-liquid or no-vapor products leads to complex steady-state behavior. Twenty-five bifurcation diagrams are presented, exhibiting a maximum of three steady states and five feasibility boundaries. Singularity theory is used to divide the Damköhler number−heat input space into regions with qualitatively different behavior for liquid, vapor, and vapor−liquid feeds. Further, it is shown that large heat of reaction, activation energy, and reactant volatility enlarge the range of operating parameters for which multiple states exist.

Introduction

Combining reaction and distillation into one apparatus is an old idea that has gained renewed interest in the recent years.[1] This combination gives rise to strongly nonlinear behavior, and the reactive distillation units may display multiple steady states. State multiplicity might lead to start-up complications,[2] undesired transitions between steady states,[2] oscillatory behavior,[3] and difficult control.[4] State multiplicity has been demonstrated in a variety of reactive distillation processes, for example, synthesis of methyl *tert*-butyl ether (MTBE), ethyl *tert*-butyl ether, *tert*-amyl methyl ether (TAME), ethylene glycol, or methyl acetate. The reader is referred to work by Güttinger and Morari[5] and Taylor and Krishna[7] for more comprehensive reviews of the relevant literature. The latter paper gives also an overview of modeling and design issues.

To analyze state multiplicity in reactive distillation, several approaches were employed. Regions of multiple solutions could be identified by tracing the dependence of the steady-state solution upon one varying parameter.[2,3,8−13] Aiming for an understanding of the multiplicity mechanism, Güttinger and Morari[5,6] assumed chemical and phase equilibrium in an infinitely long column operated at infinite reflux and applied the ∞/∞ analysis. Mohl et al. took a different approach.[2] For the TAME synthesis, they compared an isothermal continuous stirred tank reactor (CSTR) and reactive distillation units having different numbers of stages. The same type of behavior was found. Therefore, the authors concluded that multiple steady states are caused by kinetic instabilities. Gehrke and Marquardt[14] brought together reaction and distillation into a one-stage process. The reaction kinetics was accounted for. The system was analyzed by a singularity theory approach. Qualitatively similar behaviors were obtained for one- and multiple-stage columns. The existence of feasibility boundaries was outlined, but this aspect was not detailed. Rodriguez et al. employed an even simpler model, the isobaric adiabatic reactive flash.[15,16] They showed that multiplicity is caused by the interaction between separation and reaction in systems in which the activation energy and the gradient of the boiling temperature with composition are sufficiently large. Because vapor−liquid equilibrium can create multiple steady states, state multiplicity becomes possible in endothermic or slightly exothermic systems, which typically do not display multiplicity in a one-phase CSTR. Several examples were considered, and parametric studies were performed. In addition, for an isomerization reaction, necessary conditions for multiplicity were derived. These conditions are somehow difficult to apply because they are expressed in terms of system properties such as the heat of vaporization or heat of reaction but also include, however, the unknown liquid- and vapor-phase compositions.

In the present paper, we approach the reactive flash from a different perspective. We employ a dimensionless model and distinguish the state variables, as liquid and vapor compositions, from system properties such as the heat of reaction or activation energy and control parameters such as the feed rate or heat duty. Aiming to uncover the possible behavior patterns, we present 25 bifurcation diagrams that are qualitatively different. We demonstrate the importance of the feasibility boundaries corresponding to no-liquid or no-vapor products, illustrated in bifurcation diagrams exhibiting three and even five such points. Further, we show that high heat of reaction, activation energy, and reactant volatility enlarge the range of operating parameters for which multiple states exist.

This paper is organized as follows. We start by presenting the reactive-flash model, which is used to introduce the singular points where the number of steady states changes. Then, a dimensionless model is derived and discussed. In the following section, we choose a base case characterized by small heat of reaction, moderate activation energy, and high relative volatility of the reactant. Focusing on the effect of control parameters, we identify the main types of

* To whom correspondence should be addressed. Tel.: +31 15 278 6076. Fax: +31 15 278 4370. E-mail: c.s.bildea@tnw.tudelft.nl.

10.1021/ie0488748 CCC: $30.25
Published on Web 04/14/2005

behavior occurring in large regions of the parameter space and the important varieties bounding these regions. Afterward, we investigate the effect of system properties such as the heat of reaction, activation energy, and relative volatility. The paper ends with conclusions.

Model

Figure 1 shows the flowsheet of a reactive flash. Pure reactant, preheated to temperature T_0 and contains the vapor fraction ϵ, is fed with the flow rate F. The first-order isomerization reaction A → B takes place in the liquid phase only, which is assumed to be well mixed. A level controller maintains the liquid holdup M by manipulating the liquid flow rate L. Vapor removal rate V is adjusted by the pressure controller. Heat is added or removed at the rate Q. $z = 1$, x, and y are the reactant mole fractions in the feed and two product streams, respectively. Additionally, we assume ideal gas and liquid behavior, vapor pressures following the Antoine equation, and the same heat of vaporization for both components.

The steady-state behavior of the process can be described by eqs 1−5:

$$F - L - V = 0 \tag{1}$$

$$Fz - Lx - Vy - k_0 Mx \exp(-T/T_A) = 0 \tag{2}$$

$$xP_1^{sat} + (1 - x)P_2^{sat} - P = 0 \tag{3}$$

$$yP = xP_1^{sat} \tag{4}$$

$$k_0 Mx \exp(-T/T_A)(-\Delta H_r) - V\Delta H_{vap} + FC_p(T_0^* - T) + Q = 0 \tag{5}$$

where

$$\ln P_i^{sat} = A_i - \frac{\Delta H_{vap}}{RT} \tag{6}$$

$$T_0^* = T_0 \qquad \text{for a liquid feed } (T_0 < T_{b,A}) \tag{7a}$$

$$T_0^* = T_{b,A} + \epsilon\frac{\Delta H_{vap}}{C_p} \qquad \text{for a liquid−vapor feed } (T_0 = T_{b,A}) \tag{7b}$$

$$T_0^* = T_{b,A} + \frac{\Delta H_{vap}}{C_p} + \frac{C_{p,g}}{C_p}(T_0 - T_{b,A}) \qquad \text{for a vapor feed } (T_0 > T_{b,A}) \tag{7c}$$

The model unknowns are the temperature T and flow rate and composition of the liquid (L, x) and vapor (V, y) products. The validity of the reactive-flash model is limited by the boundaries $V = 0$ and $L = 0$. The model parameters can be divided into system-specific (k_0, T_A, ΔH_r, ΔH_{vap}, A_i, B_i, and C_p) and control parameters (M, T_0^*, F, Q, and P). Typical system properties[15] are presented in Table 1. A small heat of reaction is considered here. Rodriguez et al.[15,16] proved that, for a simple reaction rate law, there can only be one steady state if the reactant is the heavy component. Therefore, we consider a light-boiling reactant.

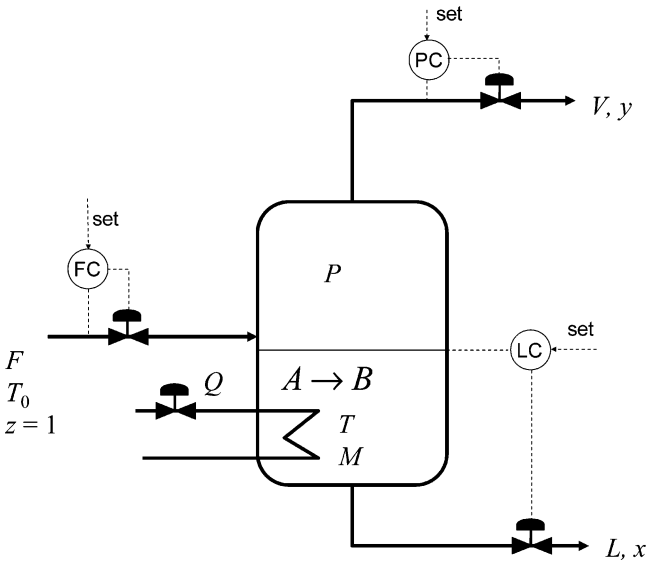

Figure 1. Reactive flash.

Table 1. System Properties

system property	dimensional variable	dimensionless variable
preexponential factor	$k_0 = 5.88 \times 10^{10}$ s^{-1}	
Arrhenius temperature	$T_A = 7300$ K	$\gamma = 30$
Antoine coefficients	$A_1 = 9.784$	$a_1 = 9.784$
	$A_2 = 7.704$	$a_2 = 7.704$
heat of vaporization	$\Delta H_{vap} = 4807$ kcal kmol^{-1}	
heat capacity	$C_p = 20.0$ kcal kmol^{-1} K^{-1}	$\lambda^{-1} = 1$
heat of reaction	$\Delta H_r = 500$ kcal kmol^{-1}	$B = 0.1$

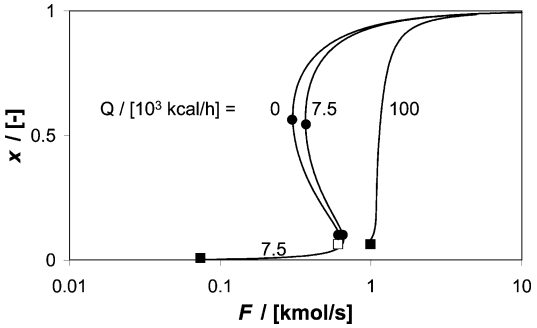

Figure 2. Liquid composition vs feed flow rate, for different values of the heat duty: $M = 5$ kmol; $\epsilon = 0.13$; ●, turning point; ■, $L = 0$ feasibility boundary; □, $V = 0$ feasibility boundary.

From the model parameters, we choose F as a *distinguished* one and use it to plot (Figure 2) the dependence of the liquid composition x, for a vapor−liquid feed ($\epsilon = 0.15$ and $T_0^* = 280$ K) and different values of the heat duty Q. The plots, called *bifurcation diagrams*, are qualitatively different. For the adiabatic case ($Q = 0$), no feasible solution exists for small F. For increasing F, the number of steady states changes from 0, to 2, 3 (small range) and 1. Note that the lower branch of the diagram starts at the feasibility boundary $V = 0$ and the diagram exhibits two *turning* points, also known as *limit* or *fold*. The second plot corresponds to a small heat duty. In this case, the lower branch starts at the boundary $L = 0$ and the multiplicity pattern is 0−1−3−1. Finally, for a large value of the heat duty, a single steady state is possible beyond the boundary $L = 0$. For each plot in Figure 2, the turning points and feasibility boundaries correspond to certain values of one parameter, the feed flow rate F. We say that these are

codimension-one bifurcation or *singular* points. We also note that the type of diagram depends on the number and relative location of the turning points and feasibility boundaries. In this paper, we will apply the singularity theory[17] to divide the space of model parameters into regions with qualitatively different bifurcation diagrams. However, aiming at general results, we will first write the model in a dimensionless form. This ensures that the number of parameters is kept to a minimum while the type of behavior predicted by the model is preserved.

Equations 1−5 can be rewritten in terms of dimensionless variables and parameters as follows:

$$l + v - f = 0 \tag{8}$$

$$fz - lx - vy - (Da)x \exp\left(\frac{\gamma\theta}{1+\theta}\right) = 0 \tag{9}$$

$$xp_1^{\text{sat}} + (1-x)p_2^{\text{sat}} - p = 0 \tag{10}$$

$$yp = xp_1^{\text{sat}} \tag{11}$$

$$f(\theta_0^* - \theta) + (Da)Bx \exp\left(\frac{\gamma\theta}{1+\theta}\right) - v\lambda + q = 0 \tag{12}$$

with

$$p_i^{\text{sat}} = \exp\left(a_i \frac{1 - b_i + \theta}{1+\theta}\right) \tag{13}$$

$$\theta_0^* = \theta_0 \qquad \text{for a liquid feed } (\theta_0 < 0) \tag{14a}$$

$$\theta_0^* = \epsilon\lambda \qquad \text{for a liquid−vapor feed } (\theta_0 = 0) \tag{14b}$$

$$\theta_0^* = \lambda + \frac{C_{\text{p,g}}}{C_{\text{p}}}\theta_0 \qquad \text{for a vapor feed } (\theta_0 > 0) \tag{14c}$$

The model contains

(i) state variables:

$$x;\ y;\ \theta = (T - T_{\text{ref}})/T_{\text{ref}};\ l = L/F_{\text{ref}};\ v = V/F_{\text{ref}}$$

(ii) physical and kinetic properties:

$$B = \frac{-\Delta H_{\text{r}}}{C_{\text{p}}T_{\text{ref}}};\ \lambda = \frac{RA_1}{C_{\text{p}}};\ \gamma = \frac{T_{\text{A}}}{T_{\text{ref}}};\ a_1 = A_1,\ a_2 = A_2;\ b_1 = 1,\ b_2 = \frac{A_1}{A_2}$$

(iii) control parameters:

$$f = F/F_{\text{ref}};\ q = \frac{Q}{F_{\text{ref}}C_{\text{p}}T_{\text{ref}}};\ Da = k(T_{\text{ref}})\frac{M}{F_{\text{ref}}};\ \theta_0^* = \frac{T_0^* - T_{\text{ref}}}{T_{\text{ref}}};\ p = P/P_{\text{ref}}$$

The boiling point of component A is used as the reference temperature. For an existing design, the nominal values of the feed flow rate and pressure would be the usual choices of the reference flow rate and pressure, respectively. Therefore, we are mainly interested in regions around $f = 1$ and $p = 1$. Note that the dimensionless model is written such that the operational parameters F, Q, $Mk(T_{\text{ref}})$, T_0^*, and P enter only in one dimensionless parameter (f, q, Da, θ_0^*, and p, respectively).

Steady-State Behavior: Effect of the Control Parameters

As previously mentioned, we choose the feed flow rate f as the distinguished parameter. By steady-state classification, we mean dividing the space of the remaining parameters into regions with qualitatively different bifurcation diagrams. To deal with the large number of parameters involved, we adopt the following strategy. First, we achieve the classification in the $Da-q$ space for a system characterized by small heat of reaction, moderate activation energy, and high relative volatility. For a vapor−liquid feed, we identify the main types of behavior occurring in large regions and the important varieties bounding these regions. Afterward, the effect of the feed condition θ_0^*, the remaining control parameter, is investigated. Finally, we look at the effect of larger heat of reaction, larger activation energy, and lower relative volatility.

Singularity theory states that the qualitative features of the bifurcation diagram may change only when the parameter set crosses the *hysteresis*, *isola*, or *double-limit* varieties.[18] Only the hysteresis variety is found for the reactive flash. When the hysteresis variety is crossed, the number of possible steady states changes by two, as two turning points appear or disappear. The defining conditions of the hysteresis variety are presented, for example, by Kuznetsov.[19]

When feasibility boundaries exist, the bifurcation diagram may also change at special sets of parameters.[17] In this work, we considered the following:

(i) The *boundary-limit set*: a turning point occurs at a feasibility boundary.

(ii) The *boundary-tangent set*: the bifurcation diagram is tangent to the feasibility boundary. After crossing this set, the bifurcation diagram changes by appearance/disappearance of two feasibility boundaries.

(iii) The *cross-and-limit set*: the position of one turning point relative to one solution located at the feasibility boundary changes.

(iv) The *corner set*: the bifurcation parameter and the state variable are, simultaneously, at their boundaries.

The above-mentioned varieties are said to be of codimension two because their defining conditions can be solved for the state variables and two parameters (for example, f and q).

The dynamic model of the reactive flash contains several algebraic equations, but only one differential equation, when the holdup and pressure are fixed and the phase equilibrium is instantaneous. Such one-dimensional systems cannot exhibit Hopf bifurcations, leading to oscillatory behavior. Therefore, dynamic classification is not necessary.

Heat Duty. For a better understanding of the steady-state classification, we present in Figure 3 the loci of codimension-one singular points in a $f-q$ plot. Note that these points are introduced in Figure 2. Because $f-x$ bifurcation diagrams are obtained for a given value of the q parameter, the number and relative location of singular points can be obtained by the intersection of q = *constant* horizontal lines with the locus of codimension-one singular points. At large q, there is only one intersection with the boundary $l = 0$, and the bifurcation

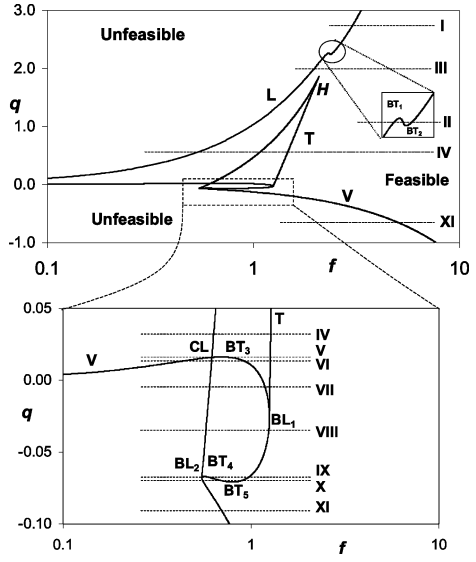

Figure 3. Codimension-one singular points: $Da = 0.10$; $p = 1$; $\theta_0^* = 0.13$; T, turning point; V and L, feasibility boundaries corresponding to $v = 0$ and $l = 0$, respectively; H, cusp; BT, boundary tangent; CL, cross-and-limit; BL, boundary limit. Qualitatively different bifurcation diagrams corresponding to regions I–XI are shown in Figure 4. Physical properties are given in Table 1.

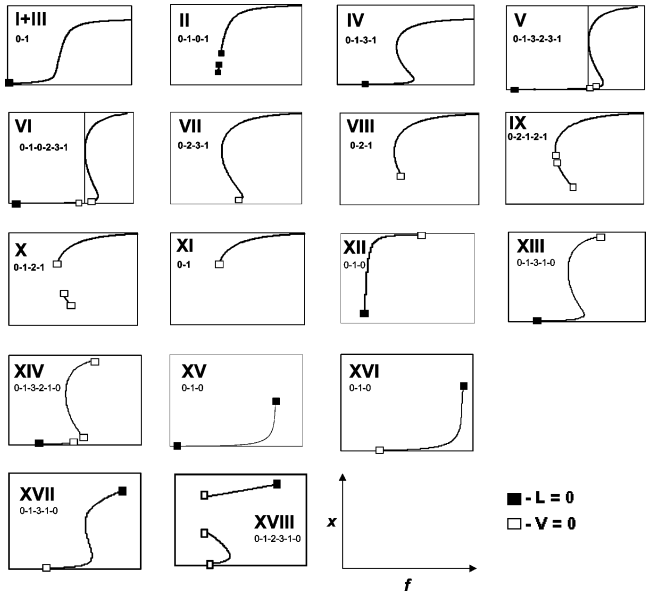

Figure 4. Qualitatively different bifurcation diagrams. Diagrams I–XI correspond to regions I–XI in Figures 3 and 5. Diagrams XII–XVIII correspond to regions XII–XVIII in Figure 7.

diagram is similar to the case $Q = 10^5$ kcal h^{-1} in Figure 2 or diagrams I + III in Figure 4. Upon a decrease in q, a narrow region with three $l = 0$ boundaries is encountered. This region is bounded by the local extremes of the q vs f plot, which are the boundary-tangent points BT_1 and BT_2. Diagram II is representative for the behavior in this region. Upon a further decrease in q, two turning points are met below the cusp H. State multiplicity becomes possible, as shown in diagram IV of Figure 4. Note that the hysteresis represents the locus of cusp points. Many changes occur within a small region around $q = 0$, which is detailed in a close-up. First, the boundary-tangent set BT_3 is crossed to region V, leading to two $v = 0$ boundaries. Immediately, the relative locations of a turning point and a $v = 0$

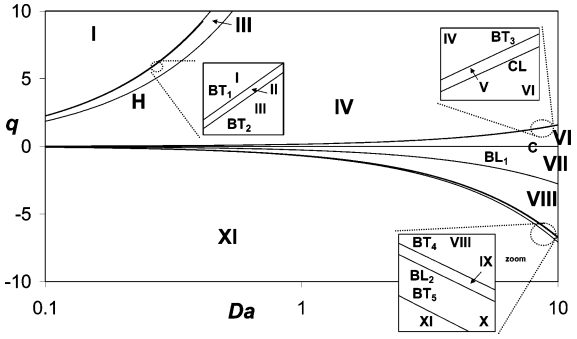

Figure 5. Steady-state classification of the reactive-flash model: $p = 1$; $\theta_0^* = 0.13$; H, hysteresis; C, corner set; BT, boundary-tangent set; CL, cross-and-limit set; BL, boundary-limit set. Bifurcation diagrams corresponding to regions I–XI are shown in Figure 4. Physical properties are given in Table 1.

feasibility boundary change at a cross-and-limit point CL, leading to diagram VI. Upon a further decrease in q to region VII, the $v = 0$ and $l = 0$ boundaries move toward $f = 0$ and disappear at corner points (not shown). One turning point leaves the feasible domain at the boundary limit BL_1, and the maximum number of steady states becomes two, as in diagram VIII. Finally, the other turning point becomes infeasible, and the state multiplicity disappears (region XI). We also note a very narrow range of q values where three $v = 0$ boundaries exist (diagrams IX and X).

Damköhler Number. The steady-state classification is achieved by computing the codimension-two points for different values of an additional parameter, the Damköhler number. In this way, the Da–q space is divided into several regions (Figure 5). The different f–x bifurcation diagrams existing in each region are shown in Figure 4. Note that some regions (II, V, IX, and X) are very small.

Feed Condition. In the previous section, we looked at the steady-state behavior of the reactive-flash model for a vapor–liquid feed ($0 < \theta_0^* < 1$). All of the bifurcation diagrams of Figure 4 show a feasible steady state for large values of the feed flow rate. Among them, the diagrams consisting of two disconnected branches and containing three feasibility boundaries should be remarked upon. Such diagrams are born when boundary-tangent sets are crossed. The diagrams are found, however, in narrow regions of the Da–q space. In this section, we will show that, when the feed is a subcooled liquid ($\theta_0^* < 0$) or an overheated vapor ($\theta_0^* > 1$), the reactive-flash model has feasible steady states only over a finite range of heat duty. Moreover, the boundary-tangent sets become more important for the classification of the steady-state behavior.

The top plot of Figure 6 shows the location of the $v = 0$ boundary for values of the θ_0^* parameter around $\theta_0^* = 0$. Compared to Figure 4, the boundary-tangent sets BT_3 and BT_5 disappear when the vapor fraction increases to $\theta_0^* = 0.3$ and the feed is a subcooled liquid of $\theta_0^* = -0.2$, respectively. However, the distance between the two boundary-tangent sets becomes larger, which is reflected by larger regions where the bifurcation diagram consists of two disconnected branches separated by $v = 0$ points. The shape of the $l = 0$ boundary changes around $\theta_0^* = \lambda = 1$ (second plot of Figure 6), where the set BT_2 disappears. The set BT_1 disappears only for higher values of θ_0^*. We also note that, for vapor-only or

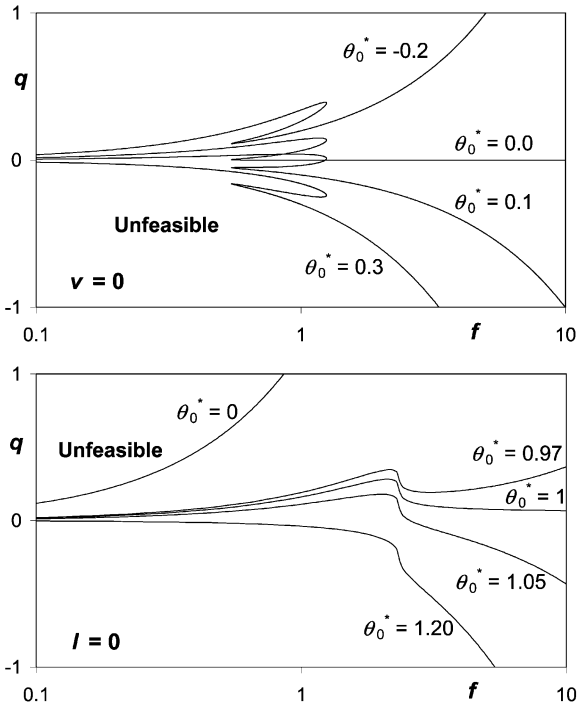

Figure 6. Effects of the feed condition on the feasibility boundaries: $Da = 0.10$; $p = 1$. Physical properties are given in Table 1.

liquid-only feeds, the $f-x$ bifurcation diagrams show at least one $v = 0$ and one $l = 0$ boundaries.

Phase diagrams for three different feed conditions are presented in Figure 7, where only the large regions are shown. For a liquid feed ($\theta_0^* = -0.2$), a vapor product is possible only if the heat of reaction is sufficient to generate vapors. At low Da and large q (region XIIa), the $f-x$ bifurcation diagrams show a single steady state. The solution branch starts at $l = 0$ boundary and ends at the $v = 0$ boundary. When the hysteresis is crossed to region XIII, multiple steady states occur. When the boundary-tangent set BT_3 is crossed to region XIV, two new $v = 0$ boundaries appear. By moving further to region XIIb, the bifurcation diagram shows again a single branch due to the coalescence of the middle and high $v = 0$ boundary at the boundary-tangent set BT_4.

For a vapor feed ($\theta_0^* = 1.1$), the feasibility of the model is bounded by the set BT_1. At large Da (region XVIa), the $f-x$ bifurcation diagrams show a single steady state, starting at the $v = 0$ boundary and ending at the $l = 0$ boundary. In region XVII, state multiplicity exists. When the boundary-tangent set BT_4 is crossed to region XVIII, two new $v = 0$ boundaries appear. By moving further to region XVIb, the bifurcation diagram shows again a single branch, after the low and middle $v = 0$ boundaries disappear at the boundary-tangent set BT_5. If the feed is further heated (for example, $\theta_0^* = 1.2$), region XV disappears and a liquid product can be obtained only if heat is removed ($q < 0$).

Steady-State Behavior: Effect of the System Properties

In the following, the effect of the heat of reaction, activation energy, and relative volatility on the steady-state behavior of the reactive flash will be described. Note that modifying the heat of vaporization would change more than one dimensionless parameter because it was used to define the reference temperature. The

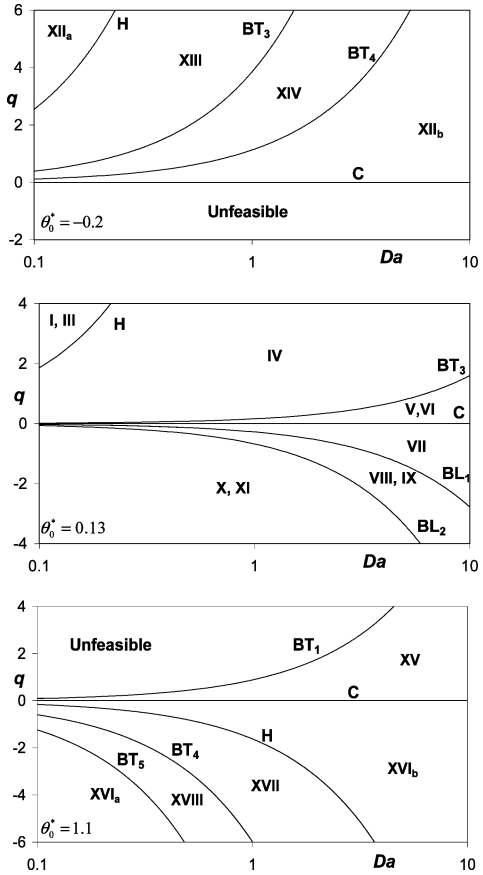

Figure 7. Influence of the feed condition on the steady-state classification: $p = 1$; H, hysteresis; BL, boundary limit; C, corner set; BT, boundary tangent; a, upper branch; b, lower branch. Bifurcation diagrams corresponding to regions I–XVIII are shown in Figure 4. Physical properties are given in Table 1.

system analyzed in the previous section (Table 1) will be labeled as the "reference case". We do not aim to give a complete classification with respect to physical properties, because of the large amount of details that are involved. However, trends that occur in the steady-state behavior are addressed. New types of bifurcation behavior that are revealed during the analysis are given in Figure 13.

Heat of Reaction. In this section, the effect of the heat of reaction on the steady-state behavior of the reactive flash is examined. The reference-case parameters are used, except the adiabatic temperature rise B. The hysteresis variety moves to lower values of Da and higher values of q upon an increase in the heat of reaction, leading to a larger area of state multiplicity. However, the area of multiplicity does not disappear when the heat of reaction is reduced to zero.

Figure 8 shows the feasibility boundaries for large heat of reaction and different values of the feed condition θ_0^*. Compared to Figure 6, the feasibility boundaries have a different shape and are located at lower values of the heat input q. The explanation is straightforward: as more heat is generated by the reaction, less heat has to be added to the system to vaporize the entire feed ($l = 0$) or to generate vapors from a given feed ($v = 0$). Moreover, we can still recognize the $\theta_0^* = 0$ and $\theta_0^* = \lambda$ limiting cases.

Figure 9 shows the loci of codimension-one points in the $f-q$ space. As the heat of reaction B is increased, the cusp crosses the feasibility limit $l = 0$ at a codimension-three point and moves into the infeasible region.

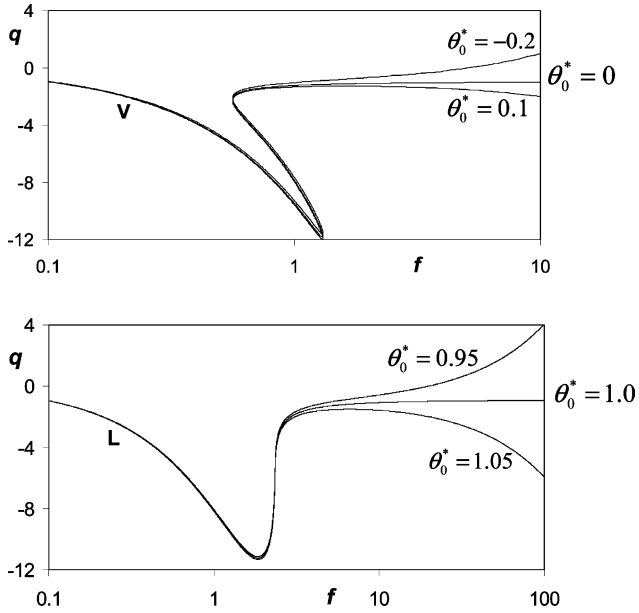

Figure 8. Effect of the feed condition on the feasibility limits for large heat of reaction: $B = 10$; V and L, feasibility boundaries corresponding to $v = 0$ and $l = 0$; $Da = 0.10$; $p = 1$.

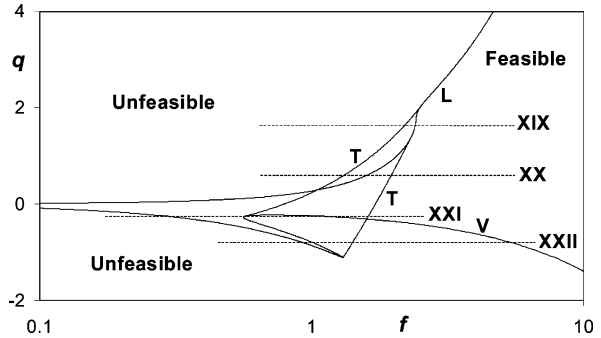

Figure 9. Codimension-one singular point for large heat of reaction: $B = 1$; $Da = 0.10$; $p = 1$; $\theta_0^* = 0.13$.

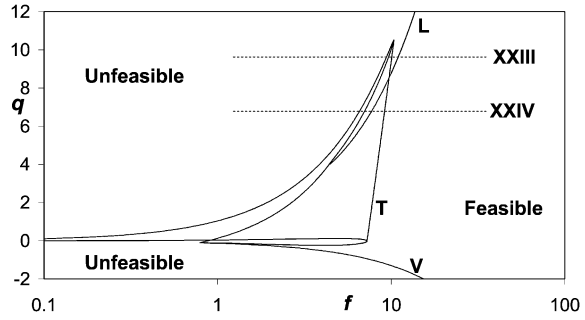

Figure 10. Codimension-one singular points for large activation energy: $Da = 0.10$; $p = 1$; $\theta_0^* = 0.13$; $\gamma = 40$; T, turning point; V and L, feasibility boundaries corresponding to $v = 0$ and $l = 0$, respectively.

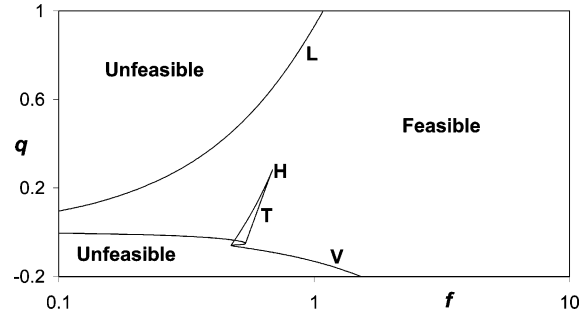

Figure 11. Codimension-one singular points for smaller relative volatility, $\alpha = 4.5$: $Da = 0.10$; $p = 1$; $\theta_0^* = 0.13$; T, turning point; H, hysteresis variety; V and L, feasibility boundaries corresponding to $v = 0$ and $l = 0$, respectively.

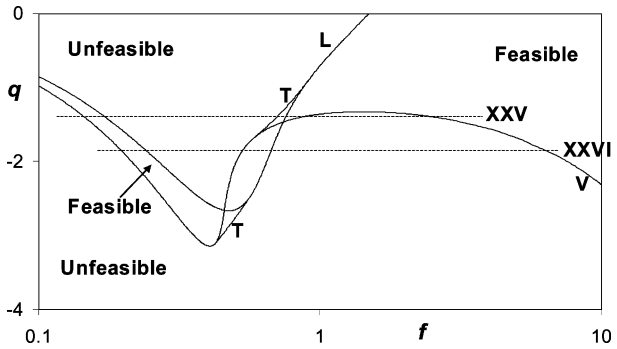

Figure 12. Codimension-one bifurcation points for small relative volatility, $\alpha = 2.0$: $Da = 0.10$; $p = 1$; $\theta_0^* = 0.13$; $B = 10$; $\gamma = 50$; T, turning point; V and L, feasibility boundaries corresponding to $v = 0$ and $l = 0$, respectively.

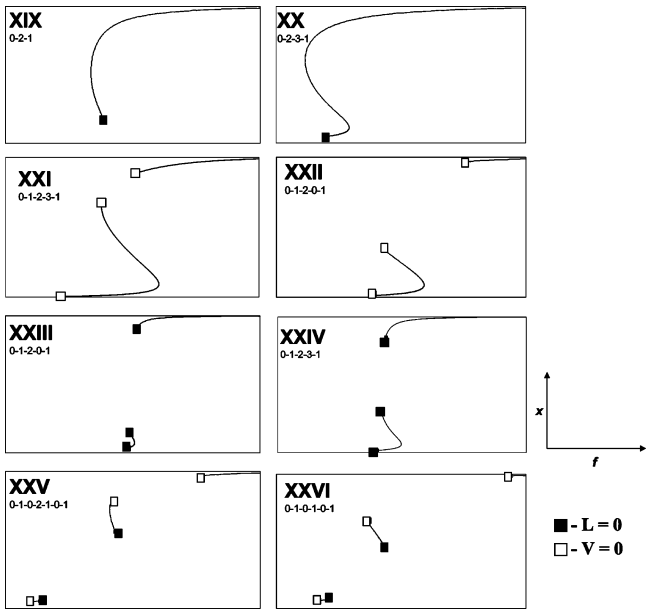

Figure 13. Bifurcation diagrams found for large heat of reaction and large activation energy.

Although the area between the loci of the turning points is partly in the infeasible region, not all branches of the bifurcation diagram are infeasible. These changes result in new types of bifurcation diagrams, XIX, XX, XI, and XXII, which are illustrated in Figure 13.

Activation Energy. In this section, the effect of increasing the activation energy on the steady-state behavior of the reactive flash is described. An illustrative plot is given in Figure 10, where the loci of turning points and feasibility limits $v = 0$ and $l = 0$ are given in the $f-q$ space. From Figure 10, it is clear that larger activation energy results in a significantly larger area of multiplicity. The cusp point is not shown because it is not physically feasible ($l < 0$). Furthermore, the extremes in the feasibility boundaries are further apart from each other. Therefore, the regions with bifurcation diagrams having three feasibility boundaries become larger and more relevant.

Relative Volatility. In the reference case, the relative volatility $\alpha = 8$ had a large value. As demonstrated

by the study of an ethylene glycol reactive distillation column, high volatility contributes to state multiplicity.[8] This section investigates the effect of lower relative volatility.

Figure 11 shows the feasibility boundaries and the locus of the turning points if α is reduced from α = 8 to 4.5. The extent of the multiplicity region is smaller. Moreover, the feasibility boundaries are less relevant because the extremes of the $l = 0$ boundary disappeared and the region between the turning points of the $v = 0$ line is quite small.

Figure 12 illustrates the behavior when low relative volatility is combined with large heat of reaction and activation energy. Although the area of multiplicity is still small, the feasibility boundaries are more significant. For example, bifurcation diagrams XXV and XXVI with five feasibility boundaries can be observed.

Conclusion

The classification of the steady-state behavior of a reactive flash is presented for a system with a mildly exothermic isomerization reaction and a light-boiling reactant. The number and relative location of the turning points and feasibility boundaries corresponding to no-liquid or no-vapor products determine the qualitative nature of the bifurcation diagram. State multiplicity is present in a large area of the parameter space, for the considered case. A total of 25 qualitatively different bifurcation diagrams can be identified for the system. The feasibility boundaries play an important role in the classification of the reactive flash. Up to five feasibility boundaries and a maximum of three steady states are found in a single bifurcation diagram. Bifurcation diagrams exhibiting more than two feasibility boundaries are common for a liquid or vapor feed. Increasing the heat of reaction, activation energy, or relative volatility enlarges the area of multiplicity. Furthermore, a large heat of reaction can create regions in parameter space with five feasibility boundaries in a single bifurcation diagram.

The singularity theory approach could be useful to investigate the main behavior patterns in more complex reactive distillation systems, including multicomponent, multireaction, and nonideal systems. The effect of mass transfer would be interesting to examine. Higler et al.[20] compared both models for a MTBE system and concluded that the results of a mass-transfer model show significant quantitative differences from an equilibrium model but that multiplicity exists for both models. Finally, the model of the reactive flash could be extended with nonreactive trays, including a condenser and reboiler.

Acknowledgment

The financial support of the European Commission (Research Training Network MRTN-CT-2004-512233, "Towards Knowledge-Based Processing Systems") is gratefully acknowledged.

Nomenclature

A_i = Antoine coefficient of component i
a_i = dimensionless Antoine coefficient of component i
B = dimensionless heat of reaction
B_i = Antoine coefficient of component i [K]
b_i = dimensionless Antoine coefficient of component i
C_p = heat capacity of the liquid [kcal kmol^{-1} K^{-1}]
Da = Damköhler number
F = feed flow rate [kmol s^{-1}]
f = dimensionless feed flow rate
P = pressure [atm]
p = dimensionless pressure
k_0 = preexponential factor [s^{-1}]
L = liquid flow rate [kmol s^{-1}]
l = dimensionless liquid flow rate
M = molar holdup [kmol]
Q = external heat source [kcal s^{-1}]
q = dimensionless external heat source
R = gas constant [kcal kmol^{-1} K^{-1}]
r = reaction rate [s^{-1}]
T = temperature [K]
V = vapor flow rate [kmol s^{-1}]
v = dimensionless vapor flow rate
x = liquid molar fraction of component A
y = vapor molar fraction of component A
ΔH_r = heat of reaction [kcal kmol^{-1}]
ΔH_{vap} = heat of vaporization [kcal kmol^{-1}]

Greek Letters

α = relative volatility
γ = dimensionless activation energy
ϵ = vapor fraction in the feed
λ^{-1} = dimensionless heat capacity
θ = dimensionless temperature

Subscripts

0 = inlet
A = component A
b = boiling conditions
g = gas
i = component
ref = reference

Superscripts

sat = saturated
* = feed condition

Literature Cited

(1) Malone, M. F.; Doherty, M. F. Reactive Distillation. *Ind. Eng. Chem. Res.* **2000**, *39*, 3953.

(2) Mohl, K.; Kienle, A.; Gilles, E.; Rapmund, P.; Sundmacher, K.; Hoffmann, U. Steady-state multiplicities in reactive distillation columns for the production of fuel ethers MTBE and TAME: theoretical analysis and experimental verification. *Chem. Eng. Sci.* **1999**, *54*, 1029.

(3) Hauan, S.; Hertzberg, T.; Lien, K. M. Multiplicity in reactive distillation of MTBE. *Comput. Chem. Eng.* **1997**, *21*, 1117.

(4) Al-Arfaj, M. A.; Luyben, W. L. Comparative control study of ideal and methyl acetate reactive distillation. *Chem. Eng. Sci.* **2002**, *57*, 5039.

(5) Güttinger, T. E.; Morari, M. Predicting multiple steady states in equilibrium reactive distillation. 1. Analysis of nonhybrid systems. *Ind. Eng. Chem. Res.* **1999**, *38*, 1633.

(6) Güttinger, T. E.; Morari, M. Predicting multiple steady states in equilibrium reactive distillation. 2. Analysis of hybrid systems. *Ind. Eng. Chem. Res*. **1999**, *38*, 1649.

(7) Taylor, R.; Krishna, R. Modelling reactive distillation. *Chem. Eng. Sci.* **2000**, *55*, 5183.

(8) Ciric, A. R.; Miao, P. Steady-state multiplicities in an ethylene glycol reactive distillation column. *Ind. Eng. Chem. Res*. **1994**, *33*, 2738.

(9) Kumar, A.; Daoutidis, P. Modeling, analysis and control of ethylene glycol reactive distillation column. *AIChE J.* **1997**, *45*, 51.

(10) Baur, R.; Taylor, R.; Krishna, R. Dynamic behaviour of reactive distillation columns described by a nonequilibrium stage model. *Chem. Eng. Sci.* **2001**, *56*, 2085.

(11) Sneesby, M. G.; Tadé, M. O.; Smith, T. N. Steady-state transitions in the reactive distillation of MTBE. *Comput. Chem. Eng.* **1998**, *22*, 879.

(12) Sneesby, M. G.; Tadé, M. O.; Smith, T. N. Multiplicity and pseudo-multiplicity in MTBE and ETBE reactive distillation. *Chem. Eng. Res. Des.* **1998**, *76* (A2), 525.

(13) Chen, F.; Huss, R. S.; Doherty, M. F.; Malone, M. F. Multiple steady states in reactive distillation: kinetic effects. *Comput. Chem. Eng*. **2002**, *26*, 81.

(14) Gehrke, V.; Marquardt, W. A. singularity theory approach to the study of reactive distillation. *Comput. Chem. Eng*. **1997**, *21*, S1001.

(15) Rodriguez, I. E.; Zheng, A.; Malone, M. F. The stability of a reactive flash. *Chem. Eng. Sci.* **2001**, *56*, 4737.

(16) Rodriguez, I. E.; Zheng, A.; Malone, M. F. Parametric dependence of solution multiplicity in reactive flashed. *Chem. Eng. Sci.* **2004**, *59*, 1589.

(17) Balakotaiah, V.; Luss, D. Global analysis of the multiplicity features of multi-reaction lumped parameter systems. *Chem. Eng. Sci.* **1984**, *39*, 865.

(18) Golubitsky, M.; Schaeffer, D. G. *Singularities and groups in bifurcation theory*; Springer-Verlag: New York, 1985.

(19) Kuznetsov, Y. A. *Elements of applied bifurcation theory*; Springer-Verlag: New York, 1998.

(20) Higler, A. P.; Taylor, R.; Krishna, R. Nonequilibrium modeling of reactive distillation: Multiple steady states in MTBE synthesis. *Chem. Eng. Sci.* **1999**, *54*, 1389.

Received for review November 22, 2004
Revised manuscript received February 27, 2005
Accepted March 11, 2005

IE0488748